Improved Mobile 70 MeV Race-Track Microtron Design

V.I. Shvedunov, Institute of Nuclear Physics, Moscow State University, 119899, Moscow, Russia
A.I. Karev, Physical Institute, Russian Academy of Science
V.N. Melekhin, Institute for Physical Problems, Russian Academy of Science
N.P. Sobenin, Moscow Engineering Physics Institute
W.P. Trower, Physics\Virginia Tech, Blacksburg VA 24061 USA

To increase the reliability, simplify the tuning, and boost the efficiency of our 70 MeV mobile Race-Track Microtron design we use a narrow rectangular asymmetric accelerating structure, rare-earth permanent end magnets, wiggler-like vertical focusing lenses on the return paths, and a beam buncher preceding the linac. We present here beam dynamics simulation results and construction details.

I. INTRODUCTION

Our original 70 MeV mobile **R**ace **T**rack **M**icrotron design [1] was based on proven principles but included new features which decreased the RTM weight and size while increasing its efficiency: Beam reflection in the end magnet fringe field on the first orbit to bypass the linac followed by acceleration in the reverse direction; End magnets with main and reverse field coils optimized to reduce size and weight; Tuning of the reverse field amplitude and position; Vertical focusing by the end magnet fringe fields and internal field gradients; Horizontal focusing by an on-linac-axis quadrupole singlet; and A linac optimized for efficient low-energy beam capture and high-energy beam acceleration.

Our design, as well as those of most pulsed RTMs, had inherent problems: Precisely retro-reflecting the beam on the linac axis combined with accurate fringe field focusing; Increasing parasitic losses when the dispersed reflected beam enters linac; Achieving stable phase oscillations by adjusting both end magnet positions; Synchronous phase drift decreasing the phase stability region and increasing the number of orbits, owing to the end magnet field gradient; Decreasing the RTM efficiency and increasing the environmental radiation by beam losses (10-20 % with a specially optimized linac depending on the injected beam transverse emittance).

To solve these problems we introduce a narrow asymmetric rectangular accelerating structure [2] which, together with short-tail fringe field **R**are **E**arth **P**ermanent **M**agnet end magnets [3], allows the beam to clear the linac after the first acceleration. The beam dispersion after the first end magnet passage is compensated for by the second end magnet. The position of only one magnet need be adjusted to achieve stable phase oscillations. Our REPM end magnets, smaller than conventional electromagnets with coils, require no power supply or cooling.

We vertically focus the beam with REPM wiggler-like lenses installed on the return paths instead by end magnet field gradient. These lenses negligibly influence the horizontal motion, no synchronous phase drifts are induced, and the phase stability region is easily maximized.

Table I
RTM parameters.

Injection energy	55 keV
Energy gain per turn	5.26 MeV
Number of turns	14
Output energy	10 - 74 MeV
Output current at 70 MeV	45 mA
Increase in orbit circumference per turn	1 λ
Operating frequency	2,450 MHz
Klystron power pulsed/average	5 MW/5 (15) kW
End magnet field induction	0.9 T
RTM dimensions	2 x 0.6 x 0.6 m^3

We have placed a beam buncher at the accelerating structure entrance to increases the beam capture and decrease the beam losses. The principle RTM parameters are given in Table I and the RTM block-diagram is shown in Fig. 1.
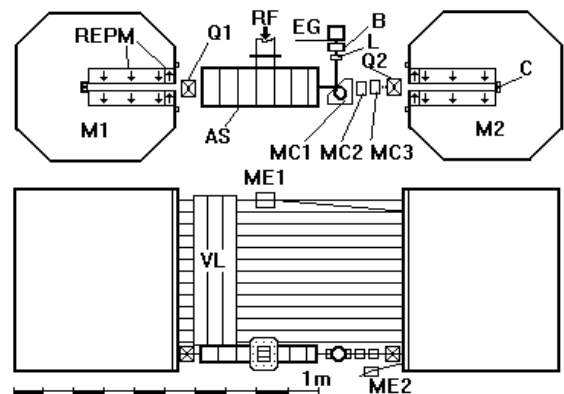

Fig. 1. RTM schematic: M1 & M2 REPM end magnets, correcting **C**oils, **A**ccelerating **S**tructure, **E**lectron **G**un, **B**uncher, **Q**uadrupole singlets, MC1-3 chicane magnets,

solenoid **L**ens, **V**ertical **L**enses, and ME1 and ME2 extraction magnets.

II. END MAGNET AND ACCELERATING STRUCTURE FOCUSING

After first acceleration and end magnet passage, an orbit's displacement from the linac axis, depends on the orbital circumference increase per turn, ν, the injection energy, the energy gain per turn, and the end magnet fringe field configuration. Injecting at several tens of keV and making $\nu = 1$ by changing the reverse field amplitude and position at the end magnet entrance, this displacement can be adjusted from zero (i.e., retro-reflection on-the-linac axis) to a value exceeding the orbit diameter in a fringe fieldless ideal end magnet. To realize the maximum orbit diameter without strong fringe field defocusing the reverse field maximum must be in as close proximity as possible to the main magnet yoke (i.e., a short-tail fringe field similar to that of ref. 4). For magnets with main and reverse coils this distance usually exceeds the reverse pole gap so that magnetic flux will not penetrate the main yoke.

The end magnet fringe field tail is shorter in our REPM end magnet [3] than in our original electromagnet with coils, as seen in Fig. 2. The REPM end magnet fringe field is focusing in the first orbit which is ~0.33 λ from the linac axis. The fringe field, whose focusing energy dependence [5] is shown in Fig. 3, is slightly defocusing for higher energies with a ~60 m focal length on the last orbit.
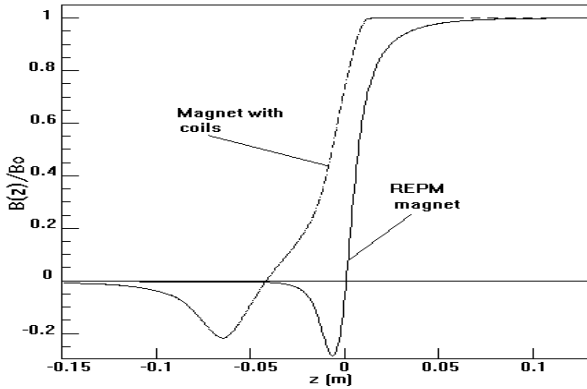

Fig. 2. End magnet fringe fields.

Our original axially symmetrical accelerating structure with optimized effective shunt impedance and operating in a E_{01}-like mode has a ~0.375 λ radius. Thus, even neglecting wall thickness, the first orbit beam would hit the accelerating structure. This radius can be decreased by capacitive loading the accelerating cells with long drift tubes, but the effective shunt impedance for adequate structure radius will at least be halved from the quality factor decrease.

We break the axial symmetry of the accelerating structure to reduce its dimensions in the orbit plane. Guided by our experience with rectangular classical microtron cavities [6] and with collider accelerating structures lacking axial symmetry [7], we use a standing wave on-axis coupled rectangular accelerating structure with circular beam holes [2]. Our calculations [8] and experiments [2] show that in the orbit plane our linac with half-width ~0.27 λ and vertical-to-horizontal dimension ratio of 2:1 has a shunt impedance 10-20% higher (~90 MΩ/m for $\lambda = 0.1224$ m) than our previous optimized axially symmetric structure.

For relativistic particles the radial electric and azimuthal magnetic field forces nearly cancel in axially symmetric structures. In an axially asymmetric structure there is a strong energy dependent quadrupole effect, focusing vertically while defocusing horizontally, as seen in Fig. 3, where the linac (one $\beta = 0.67$ cell and six $\beta = 1.0$ cells) has an on-axis voltage ratio of $U_1/U_{2\text{-}7} = 0.96$. Theoretical calculations [6] support our computer simulated results [5,8]. RTM optics compensate in the first few orbits for this strong focusing/defocusing whose strength varies directly with the accelerating structure vertical-to-horizontal dimension ratio. Our linac focusing will be further improved by using non-circular beam holes.
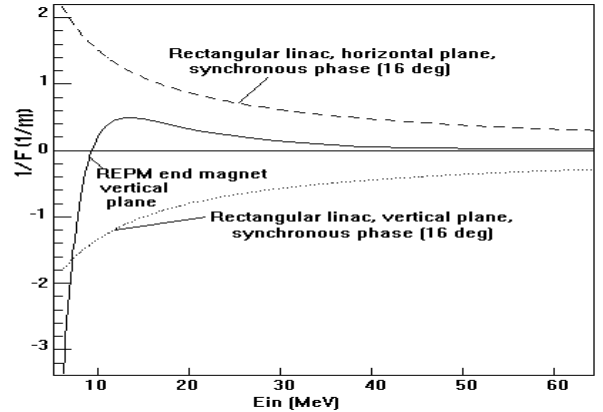

Fig. 3. REPM end magnet fringe field and rectangular linac focusing.

III. RTM OPTICS AND BEAM CAPTURE

To compensate for the horizontal linac defocusing we install a REPM quadrupole singlet, Q1, at the linac exit. The 55 keV beam injected into the linac is not focused with the energy dependence of Fig. 3 ($1/F_x = 3.1$ m^{-1}, $1/F_y = 0.97$ m^{-1} for synchronous particles) so we add a second REPM quadrupole singlet, Q2, at the end magnet M2 exit. For strong vertical focusing we use REPM wiggler-like lenses [9] at the beginning of each orbit return path. These lenses consist of three equal-length parallel-edged dipole magnets with the center dipole field doubled and reversed. The vertical focal length is $F_v = -d/4 \tan(\alpha)^2$, where α is side magnet bending angle, and d is its length chosen to be 5 cm.

The horizontal focal length is nearly infinite. The optimal bending angle range is 4°-7° and the maximum central magnet field at the last orbit is ~0.87 T. The optimal quadrupole field gradient for both lenses is ~1.75 T/m for effective length 5 cm.

Figure 4 shows that vertical and horizontal particle trajectories, displaced from the linac axis on entrance, oscillate with decreasing amplitude. In the vertical there are nonlinear effects (different vertical oscillation periods for different initial displacements) owing to end magnet fringe field.
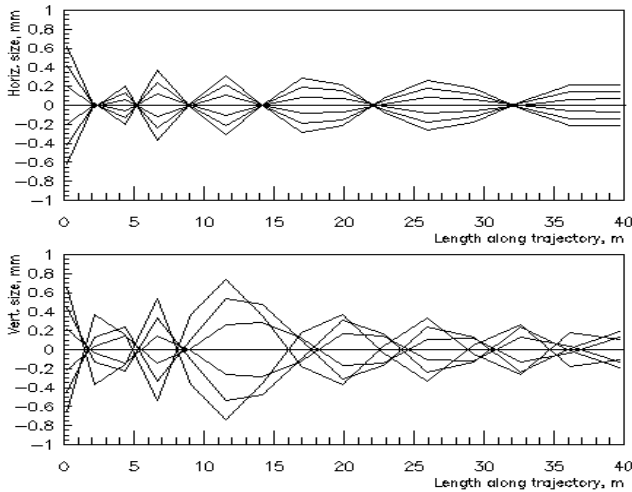

Fig. 4. Vertical and horizontal particle trajectories with displacement from the linac-axis at entrance.

To increase RTM capture efficiency and decrease parasitic beam losses we install a buncher resonator between the electron gun and the linac with buncher-linac distance of 15 cm and the buncher electric field amplitude of ~2.2% of that of the first accelerating cell. For a continuos zero transverse emittance beam there is a three-fold increase in the longitudinal capture efficiency. Otherwise the capture efficiency depends on the transverse beam emittance, its match to the RTM acceptance, and the linac injection phase. About 34% of an electron gun beam with radius x divergence of 2 mm x 10 mrad (i.e., a 80 mm x mrad transverse phase space) reaches the RTM output, twice that of our original design [1]. Thus only a ~140 mA current need be injected into the RTM to realize a 45 mA beam at exit.

Bending magnet MC1 has little influence on the longitudinal beam dynamics for the energy modulated 55 keV beam since the decreased path length for lower energy electrons is partially compensated for by their reduced velocity. However, for dispersion introduced by MC1 increases beam losses, so we inject the beam on the linac axis using a zero dispersion alpha magnet [10]. Magnets MC2 and MC3 compensate for the effect of the alpha magnet on higher orbit beams. To match the electron gun beam to the RTM acceptance we install a solenoid lens after the buncher.

IV. CONCLUSIONS

Our re-designed mobile 70 MeV pulsed race-track microtron has two essential new features -- a rectangular linac and rare-earth permanent magnets throughout --which improve its performance and efficiency.

REFERENCES

[1].N.P Sobenin, A.I Karev, V.N Melekhin, V.I Shvedunov, and W.P Trower, in *Proc. 1994 European Particle Accelerator Conf.*, V. Suller and Ch. Petit-Jean-Gernaz, editors (World Scientific, Singapore, 1994) p.512.

[2].N.P. Sobenin, V.N. Kandurin, A.I. Karev, V.N. Melekhin, V.I. Shvedunov and W.P. Trower, Rectangular Microtron Accelerating Structure, in these Proceedings.

[3].A..I. Karev, V.N. Melekhin, V.I. Shvedunov, N.P. Sobenin, and W.P. Trower, A Permanent Race-Track Microtron End Magnet, in these Proceedings.

[4].H. Babic and M. Sedlacek, *Nucl. Instr. and. Meth.* vol. 56, p.170,1967.

[5].V.G. Gevorkyan, A.B. Savitsky, M.A. Sotnikkov, and V.I. Shvedunov, VINITI, No. 183-B89 (1989) 54p. (in Russian).

[6].S.P. Kapitza and V.N. Melekhin, *The Microtron* (Harwood, London, 1978).

[7].B.V. Zverev and N.P. Sobenin, *Accelerator Structures and Resonators* (Energoatomizdat, Moscow, 1993) (in Russian).

[8].R. Klatt, F. Krawczyk, W.R. Novender, C. Palm, T. Weiland., B. Steffen, T. Barts, M.J. Browman, R. Cooper, C.T. Mottershead, G. Rodenz, and S.G. Wipf, in *Proc. 1986 Linear Accelerator Conf.*, SLAC-303 p.276 1986. A version this MAFIA code, obtained by V.S. in 1989 from T. Weiland, and installed at 586/90 was used in these calculations.

[9].L.M. Young, *IEEE Trans. Nucl. Sci.* NS-20, p.81 1973.

[10].H.A. Enge, *Rev. Sci. Instr.* vol. 34, p.385 1963.